Sequential Assembly of Cell-Laden Hydrogel Constructs to Engineer Vascular-Like Microchannels

Yanan Du,[1,2,3,4] Majid Ghodousi,[1,2,3,5] Hao Qi,[1,2,3] Nikhil Haas,[1,2,5] Wenqian Xiao,[1,2] Ali Khademhosseini[1,2,3]

[1]Department of Medicine, Center for Biomedical Engineering, Brigham and Women's Hospital, Harvard Medical School, Cambridge, Massachusetts 02139; telephone: (617)-768-8395; fax: (617)-768-8477; e-mail: alik@rics.bwh.harvard.edu

[2]Harvard-MIT Division of Health Sciences and Technology, Massachusetts Institute of Technology, Cambridge, Massachusetts

[3]Wyss Institute for Biologically Inspired Engineering, Harvard University, Boston, Massachusetts

[4]Department of Biomedical Engineering, School of Medicine, Tsinghua University, Beijing, China

[5]Department of Biomedical Engineering, Boston University, Boston, Massachusetts

ABSTRACT: Microscale technologies, such as microfluidic systems, provide powerful tools for building biomimetic vascular-like structures for tissue engineering or in vitro tissue models. Recently, modular approaches have emerged as attractive approaches in tissue engineering to achieve precisely controlled architectures by using microengineered components. Here, we sequentially assembled microengineered hydrogels (microgels) into hydrogel constructs with an embedded network of microchannels. Arrays of microgels with predefined internal microchannels were fabricated by photolithography and assembled into 3D tubular construct with multi-level interconnected lumens. In the current setting, the sequential assembly of microgels occurred in a biphasic reactor and was initiated by swiping a needle to generate physical forces and fluidic shear. We optimized the conditions for assembly and successfully perfused fluids through the interconnected constructs. The sequential assembly process does not significantly influence cell viability within the microgels indicating its promise as a biofabrication method. Finally, in an attempt to build a biomimetic 3D vasculature, we incorporated endothelial cells and smooth muscle cells into an assembled construct with a concentric microgel design. The sequential assembly is simple, rapid, cost-effective, and could be used for fabricating tissue constructs with biomimetic vasculature and other complex architectures.

Biotechnol. Bioeng. 2011;xxx: xxx–xxx.

© 2011 Wiley Periodicals, Inc.

KEYWORDS: microengineered hydrogel; directed assembly; biofabrication; biomimetic; vascular constructs

Introduction

The generation of three-dimensional (3D) vascular networks is one of the major challenges of tissue engineering (Khademhosseini et al., 2009). From a fluidic point of view, the vascular system can be deemed as a complex fluidic network comprised of the heart as a pump and a network of channels for blood transportation and distribution. As an attempt to recreate the vasculature, microscale technologies, especially microfluidic systems have emerged as promising tools for building physiological or pathological models of vasculature (Lovett et al., 2009). Microfluidics can achieve biofluidic transportation in microchannels in dimension spanning four orders of magnitude from centimeters (for larger vessels like the aorta) down to micrometers (such as a capillary) (Whitesides, 2006). The delicate control in dimension and transportation achieved by

microfluidics can be used for mechanistic understandings and therapeutic applications in cardiovascular research and tissue engineering (Andersson and van den Berg, 2004; Choi et al., 2007; Khademhosseini et al., 2006; van der Meer et al., 2009).

The necessity for an in vitro 3D vascular network has been brought about in recent years largely due to advances in the tissue engineering of complex tissue constructs (Menolascina et al., 2009). Currently, one of the major obstacles in tissue engineering is the inability to generate tissue engineered constructs with a vascular network (Hacking and Khademhosseini, 2009). Within the human body, cells are placed no further than 100–200 μm from a capillary which allows cells to receive oxygen and nutrient supplies. As a result, the lack of microvasculature in engineered tissues that are thicker than 200 μm puts a limitation on their mass transfer properties (Carmeliet and Jain, 2000). While previous works have demonstrated that cell-laden channels with diameters on the order of microns can be engineered in vitro (Chrobak et al., 2006) there is currently no method to branch large channels multi-dimensionally into consecutively smaller ones.

Most of the previous microfluidic-based vascularized systems were built by using approaches that create vascular-mimetic patterns embedded in cell-free or cell-laden bulk materials such as synthetic polymers including poly-dimethylsiloxane (PDMS), poly(lactic co-glycolic acid) (PLGA), or polyglycerol sebacate (PGS) or natural hydrogels including alginate or collagen (Borenstein et al., 2010; Choi et al., 2007; Chrobak et al., 2006; Fiddes et al., 2010; Golden and Tien, 2007; Ling et al., 2007). The vascular structures are normally in two-dimensional (2D) manner with planar vascularized patterns starting from a single channel that branches out multiple times into thinner channels. Moreover, the 2D vascularized systems usually incorporated microchannels with rectangular cross section that do not recapitulate the circular cross section of the native vessels and result in non-uniform cell seeding and unnatural cellular responses (Borenstein et al., 2010). Constructs embedded with circular cross sectioned microchannel can be formed by casting oligomer around a cylindrical template (such as a needle) (Chrobak et al., 2006; Golden and Tien, 2007) or gas stream (Fiddes et al., 2010). Despite the success of creating simple tubular lumen, none of these approaches is able to create vasculature with circular lumens mimicking the vascular network in vivo. Other approaches such as bioprinting and stereolithography have shown great promise to create 3D biomimetic branching vascular network (Jen-Huang et al., 2009; Mironov et al., 2009; Visconti et al., 2010). However the advanced facilities and expertise for biofabrication may be not readily available to common biomedical laboratories.

''Modular'' or ''bottom-up'' tissue engineering has recently emerged as a promising biofabrication approach in which shape and functional controlled microscale tissue building blocks are assembled into desirable macroscale tissue constructs (Nichol and Khademhosseini, 2009). This approach holds great potential to surpass conventional tissue engineering approaches that attempt to control the microenvironment of relatively large structures such as scaffold functionalization, especially for building complex structures with cellular scale precision (Du et al., 2008; Nichol and Khademhosseini, 2009). In this study, we present a simple approach to rapidly build cell-laden microengi-neered hydrogel (microgel) constructs embedded with vascular-like microchannels with circular lumen. We assembled an array of microgels, each with a particular architectural design, in a controlled manner in which the microchannels of each microgel were joined together upon the sequential assembly, resulting in an interconnected network mimicking the bifurcating structure of the native vasculature (Shin et al., 2004). The sequential assembly was achieved in a biphasic system, and was driven by a combination of physical manipulation, fluidic shear, and surface tension. To demonstrate the sequential assembly as a biofabrication approach, we encapsulated endothelial cells and smooth muscle cells into the microgel units with spatial arrangement mimicking the vascular physiology (Stegemann et al., 2007), which were assembled into a blood vessel-like structure. In comparison with conventional methods, our approach is simple and may provide a useful alternative for in vitro reconstruction of 3D vascular network for building vascularized tissue constructs or vascular pathological/physiological model.

Materials and Methods

All reagents were obtained from Sigma–Aldrich (St. Louis, MO), unless noted otherwise.

Fabrication of PEG Microgel Arrays

Prepolymer solution was prepared by dissolving 20% (wt/wt) poly(ethylene glycol)-diacrylate polymer [PEGDA, $M_w = 4,000$ Da; Monomer–Polymer and Daja Labs (Trevose, PA)] in Dulbecco's Phosphate Buffered Saline [DPBS; Gibco (Grand Island, NY)]. 1% photoinitiator (PI) (wt/wt), 2-hydroxy-1-(4-(hydroxyethoxy) phenyl)-2-methyl-1-propanone [Irgacure 2959; CIBA Chemicals (Tarrytown, NY)] was added to the PEGDA prepolymer solution. Photomasks of microgel arrays containing donut-shaped patterns (with inner/outer diameter of 0.5:1 mm) or more complex designs giving rise to vascular-like network and double-layers were designed by using AutoCAD and printed on transparencies with 20,000-dpi resolution [CAD/Art Services (Bandon, OR)].

A drop containing 200 μL of the photocrosslinkable PEGDA prepolymer and PI was pipetted onto a 20×26 mm^2 glass slide treated with octadecyltrichlorosilane 1% (OTS) between two glass slide spacers (150 μm thick) (Fig. 1A). A microscope cover glass slide was applied
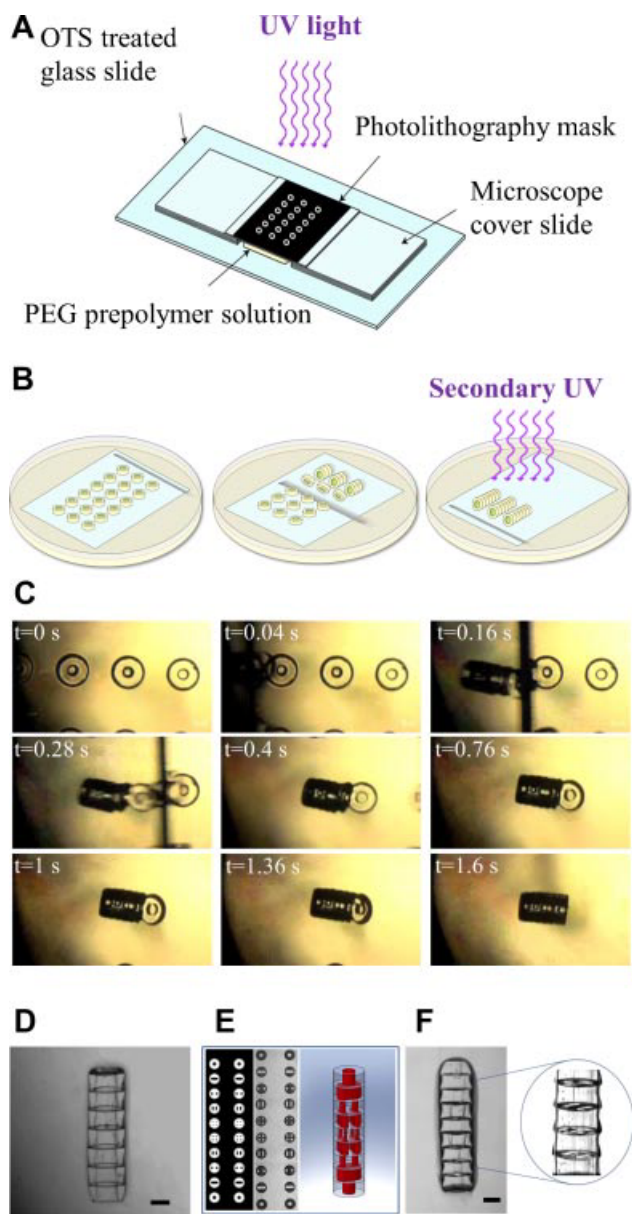
the prepolymer solution to UV light (360–480 nm; 12.4 mW/cm^2) through the photomask for 15 s.

Assembling and Stabilizing Microgels in Mineral Oil

To assemble the microgels, the glass slide with the microgel arrays was transferred to a 100×20 mm^2 Petri dish [Fisher Scientific (Pittsburgh, PA)] containing 30 mL of mineral oil [CVS Pharmacy (Boston, MA)]. The microgel arrays submerged in the mineral oil were assembled by manually swiping a $27G \times \frac{1}{2}''$ syringe needle (12.7 mm in length, BD) along the surface of the glass slide (underneath the microgel units) in the direction perpendicular to the longitude axis of the microgel arrays (Fig. 1B). As shown in the supplementary video, the swiping needle first lifted up the microgel unit from the bottom surface in a sequential manner, induced its rotation and then the fluidic shear force caused by the movements of the needle brought the hydrophilic microgels together which were further packed within the hydrophobic mineral oil (Fig. 1C). The microgel assemblies formed in mineral oil were exposed to a secondary light exposure for 10 s to crosslink and stabilize the structures. To optimize the conditions for the secondary crosslinking, prior to the assembly procedure, we washed the microgel arrays on the glass slide with PEG prepolymer or DPBS containing 1% PI or DPBS as control, respectively.

Optimization of the Assembly Process

The assembly process includes multiple stages starting from approaching the microgels with a needle, rotation of the microgels, and finally the attachment of the microgels to each other. To achieve optimal conditions for the assembly processes, the effects of five different factors on the sequential assembly of microgels were investigated including: (i) the thickness of the microgels (donut-shaped microgels with thickness of 150, 300, 450, and 600 μm); (ii) the distance between consecutive microgels on the cover slide (0.1, 0.5, and 0.9 mm); (iii) the speed of the needle ("slow": 5.5 mm/s, "medium": 9.8 mm/s, and "high": 20 mm/s) as measured by the time it took for the needle to travel a predefined distance; (iv) the diameter of the microgels (donut-shaped microgels with outer diameters of 0.5, 1, and 1.5 mm); (v) the surface tension of mineral oil on the assembly process (with addition of 0, 0.02, 0.2, and 2% of Tween 20). For each test, a number of trials were performed ($n = 19$) and the length of the assembled constructs was averaged. Optimal conditions were determined which resulted in assembled construct with the highest average length.

To analyze the mass transfer of the perfusate into the hydrogel assembly we perfused Rhodamine (0.2 mM in DPBS) through the lumen of an assembled construct and examined the lateral diffusion of the Rhodamine into the microgel by time lapse imaging. Fluorescent images were taken at a rate of 1 pic/s for a duration of 60 s.

Figure 1. Sequential assembly process of microgels using a directed assembly approach: (**A**) schematic of the microgel fabrication process; (**B**) schematic of the sequential assembly procedure: glass slide containing a prefabricated array of microgels was immersed in mineral oil and the microgels were assembled into tubular structures by swiping a needle underneath them. The assembly was subsequently stabilized by a secondary crosslinking step; (**C**) sequence of images taken of the microgels during assembly at nine different times; (**D**) phase image of the microgel tubular assembly with a single lumen; (**E**) design and phase image of the microgel arrays which should be assembled into tubular structures embedded with 3D branching lumens; (**F**) phase images of the microgel assembly with branching lumens. Scale bar: 500 μm.

on top of the solution drop, which formed an evenly distributed film of prepolymer solution between the two slides. Subsequently, a photomask was placed on the top cover slide, and microgels were formed by exposing

Viability Test of Cells Encapsulated in Microgels

To confirm that the assembly procedure could be used for biological applications, samples with encapsulated cells were collected after each step of procedure and analyzed for cell viability. NIH-3T3 cells were trypsinized and resuspended in the prepolymer solution at a concentration of 1×10^7 cells/mL. Cell-laden microgels and microgel assemblies were generated based on the optimized assembly conditions obtained from the previous section. Cell viability was characterized by Live/Dead dyes ($2\,\mu L$ of Calcein AM and $0.5\,\mu L$ of Ethidium homodimer-1; Molecular Probes, Eugene, OR) in $1\,mL$ of DPBS for $10\,min$. Cell viability was determined for cells encapsulated inside the microgles that were prepared by exposure of prepolymer solution to UV light for $15\,s$, washed with a solution containing PI, immersed in mineral oil for $30\,s$, and subsequently exposed to a secondary UV exposure for $10\,s$. All samples were incubated for $48\,h$ in cell culture medium prior to quantification of cell viability.

Building Vascular-Like Construct Containing Concentric Layers of Endothelial Cells and Smooth Muscle Cells

A two-step photolithographic method was used to fabricate concentric tubular constructs, with the internal layer labeled with Nile Red ($10\,\mu L/mL$) and outer layer labeled with $0.2\,\mu m$ green florescent microbeads ($10\,\mu L/mL$). Briefly, the outer microgel ring (OD: 1.5 mm, ID: 0.9 mm) was formed by UV exposure through the first photomask. A second photomask designed for the internal ring was aligned with the outer ring, which resulted in the formation of hydrogel ring as the internal layer (Fig. 5A). The concentric microgel arrays were assembled in oil. To mimic the physiological architecture of native vasculature, concentric microgels containing internal human umbilical endothelial cells (HUVECs) layer and outer smooth muscle cells (SMCs) layer were fabricated following the same procedure. To facilitate the visualization, SMCs were stained with PKH26 (red). Phase and florescent images were captured using an inverted fluorescent microscopy [Nikon (Melville, NY)].

Results

Sequential Assembly of Microgels into Tubular Construct

We performed sequential assembly of hydrophilic microgels in a biphasic reactor containing hydrophobic mineral oil and hydrophilic microgels. To induce the assembly a combination of surface tension and hydrodynamic interaction were used. In particular, microgel arrays containing shape-defined microgel units on a glass cover slide were first fabricated by photolithography and transferred to the mineral oil bath. The directed assembly was induced by swiping a 27G $\times$ ½″ needle uniaxially against a linear array of microgels on the glass slide. The swiping needle functioned (i) to lift the microgels off the glass slide; (ii) to produce a local shear force to rotate the microgels and (3) to drive the microgels in proximity of their neighboring microgels. The hydrophilic microgels were further packed with their immediate neighbors in the hydrophobic mineral oil resulting in cylindrical assemblies (Fig. 1D). The length and the number of the cylindrical microgel assemblies obtained from a single procedure can be determined by the number of microgels in the array, parallel and perpendicular to the swiping direction, respectively. By varying the internal designs of each individual microgel, the sequential assembly could result in microgel assembly with tubular structure or multi-luminal vascular-like network in a parallel manner (Fig. 1E and F). Figure 1E shows top-view of the photomask design (left) and phase image (middle) of the microgel arrays which generate multi-luminal microgel assembly (depicted by cartoon image in Fig. 1E (right) and phase image in Fig. 1F) upon assembly.

Optimization of the Sequential Assembly

To consistently assemble microgels into larger constructs, we systematically examined key parameters during the sequential assembly procedure including dimensions of the microgel units, distance between consecutive microgels, swiping speed of the needle, and the effect of the addition of surfactant to mineral oil (Fig. 2A).

Thickness of the Microgels

To assess the effects of microgel thickness on the assembly process, we tested microgels with four different thicknesses (150, 300, 450, and $600\,\mu m$). It was observed that sequential assembly of 300, 450, and $600\,\mu m$ thick microgels resulted in assembled constructs containing about eight microgel units on average (Fig. 2B). It was difficult to assemble thin microgels (i.e., with $150\,\mu m$ thickness), which were mechanically weak and easily damaged by the needle. Meanwhile, thick microgels (i.e., with $600\,\mu m$ and larger thicknesses) often had non-straight vertical cross sections due to the non-uniform vertical UV crosslinking under the current photolithography setup. Therefore, $450\,\mu m$ was chosen as the optimal thickness of the microgel units which were well-formed and yielded longer constructs (3.6 mm in length) upon assembly.

Diameter of the Microgels

We investigated the effect of the cross sectional diameter of the microgels on the yield of the assembly by testing microgels with diameters of 0.5, 1, and 1.5 mm. It was observed that microgels with larger diameters (corresponding to greater surface area) would result in longer assembled constructs (Fig. 2C). Sequential assembly of 0.5, 1, and
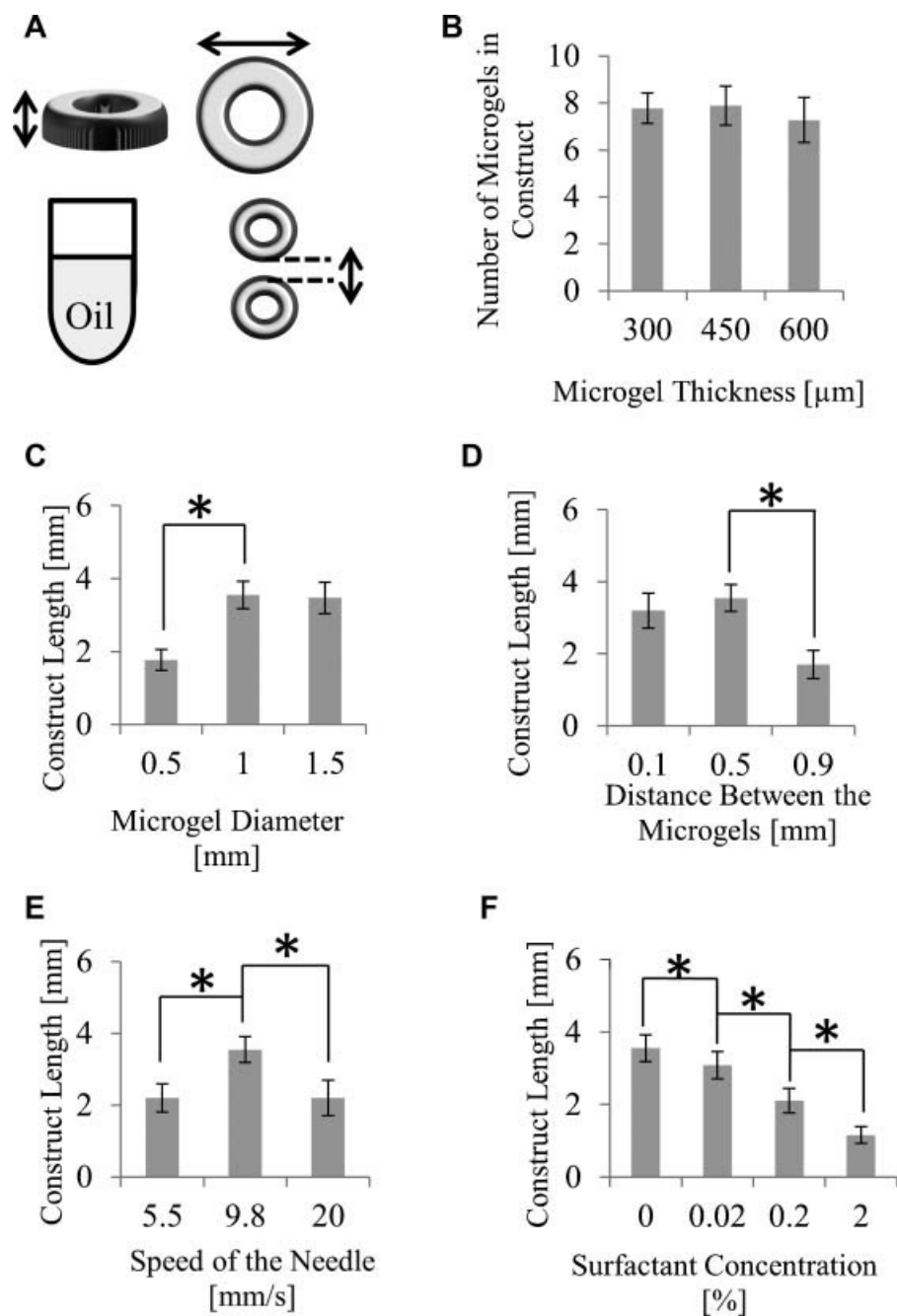
Figure 2. Optimization of the sequential assembly procedure by varying five parameters. **A**: Schematic of geometrical parameters that were modified; Effects of: **(B)** thickness of the microgel; **(C)** diameter of the microgel; **(D)** distance between two consecutive microgels on the glass slide; **(E)** swiping speeds of the needle (fast, medium, and slow); **(F)** the addition of three different amounts of surfactant to mineral oil; (significant difference among the samples ($P < 0.05$) is shown by *).

1.5 mm microgels resulted in constructs with an average length of 1.8, 3.6, and 3.5 mm, respectively. This suggests that a size of microgel's interface contact area is a deterministic factor in the assembly process. Microgels with larger diameter resulted in larger contact areas which were shown to facilitate the attachment of neighboring microgels. Meanwhile, it was observed that as the diameter of the microgels increased, larger piece of microgels effected

its proper rotation induced by the swiping needle in mineral oil and reduced the average number of microgel units within the assemblies (data not shown). Microgels with an outer diameter of 1 mm resulted in longer constructs compared to the others. We expect that it is possible to improve the sequential assembly of microgels with diameter larger than 1.5 mm using thicker needles that will have larger contact area with the microgels.

Distance Between the Microgels

Previous reports have shown that as the distance between two microgels increases, the interaction energy between them goes to zero (Shi et al., 2009). As a result, we decided to examine the effect of separation length on the length of the assembled construct. Microgel arrays with three designs were made with neighboring microgels separated (edge to edge) by three different distances (0.1, 0.5, and 0.9 mm). It was observed that microgels separated by 0.5 mm assembled to constructs with an average length of 3.6 mm that was the greatest among all (Fig. 2D). Microgels separated by 0.9 mm did not assemble properly and yielded the shortest constructs with an average length of 1.7 mm. This may be due to the long distance between the neighboring microgels that reduced the chance for the adjacent microgels to contact each other. Microgels with the smallest distance (0.1 mm) in between assembled properly but yielded shorter assembled constructs with an average length of 3.2 mm compared to microgel that were 0.5 mm apart. We therefore chose 0.5 mm as the optimal distance between the neighboring microgels in the microgel array.

Velocity of the Needle

The sequential assembly is a rapid procedure regulated by a swiping needle. Detachment of the microgels from the microscope cover slide and their rotation in mineral oil depends on the movement of the needle. Hence, the swiping speed of the needle was altered and its effects were recorded and analyzed. Swiping the needle with a medium velocity (9.8 mm/s) resulted in a construct with an average length of 3.6 mm that was the greatest among all the conditions that were tested. When the needle was swiped with a faster velocity (20 mm/s), the microgels over-rotated and assembled suboptimally and constructs with average length of 2.2 mm were obtained. When the needle was swiped with a low velocity (5.5 mm/s), the fluidic shear caused by the needle was insufficient to move the microgels in contact with each other, resulting in shorter constructs with an average length of 2.2 mm (Fig. 2E). The needle was manually manipulated in this study and can be potentially automated to enhance the efficiency.

Effects of Surfactant

Surface tension has been determined to be a major driving force of microgel assembly in mineral oil (Du et al., 2008). Hence, the surface tension of the mineral oil/water interface was altered by the addition of surfactant to the oil (0, 0.02, 0.2, and 2.0% of Tween 20 in mineral oil). It was observed that the final length of the construct varied dramatically. As surfactant concentration increased, the average length of assembled constructs decreased in a linear manner with the longest constructs being generated with a length of 3.6 mm (Fig. 2F). In our experiments, the addition of surfactant decreased the surface tension between the microgels and mineral oil. This contributed to the decreased number of microgels within the assembled constructs.

Stabilization and Perfusion of the Assembled Constructs Embedded With an Interconnected Microchannel Network

Cylindrical microgel constructs with single or multiple bifurcating channels were created by sequential assembly of microgels with specific internal design. After sequential assembly in mineral oil the cylindrical constructs were further stabilized by a secondary crosslinking. We investigated the effects of residue solution between the consecutive microgels on the secondary crosslinking. Prior to assembly, the microgel array was washed with DPBS, DPBS with 1% PI, and 10% PEG prepolymer solution with 1% PI, respectively (Fig. 3A–C). When washed by PEG prepolymer solution with PI, clogging in the lumen of the construct was observed due to the polymerization of the prepolymer solution leaking into the lumen. The assembled construct was well stabilized in the presence of 1% PI in DPBS without any visible clogging. We expect that the non-reacted acrylate groups of the PEG microgels were further crosslinked in the presence of additional PI, while the PI solution leaking to the lumen was unable to undergo self-polymerization. While using DPBS solution in the washing step could achieve stabilization of the assembly construct to some extent after secondary UV crosslinking, the stabilization was weaker compared to the PI solution and easily broken when perfusion was applied. We therefore performed UV stabilization of the tubular hydrogel construct in the presence of remaining PI solution and perfused the construct with single or multiple bifurcating lumens.

After being stabilized by secondary crosslinking, perfusion experiment was performed (see supplementary materials) to check the connectivity of the channels in the assembled construct. To facilitate the perfusion process, the assembled constructs were positioned in a custom-built perfusion chamber (Fig. 3D and E). An assembled tubular structure with simple single-channel (Fig. 3F) and another structure with multiple channels (Fig. 3G) in which a lumen with a 500 μm diameter was branched into consecutively smaller channels (as small as 100 μm in diameter) were perfused with fluorescent beads. To make the perfusion process of the construct with multiple lumens feasible, larger-diameter hydrogels with wider lumens were fabricated. These hydrogels had an outer diameter of 1.2 mm and a minimum inner diameter of 100 μm. The constructs made with the modified microgels were perfused successfully with 0.5 μm diameter florescence beads at an average flow rate of 3 μL/min.

Diffusion of nutrients and waste through the engineered construct is critical for the survival of the cells. Here we used Rhodamine dye to visualize this process in our experiments. Rhodamine dye perfused through the gels in a relatively short time (Fig. 3H). The high speed at which this dispersion
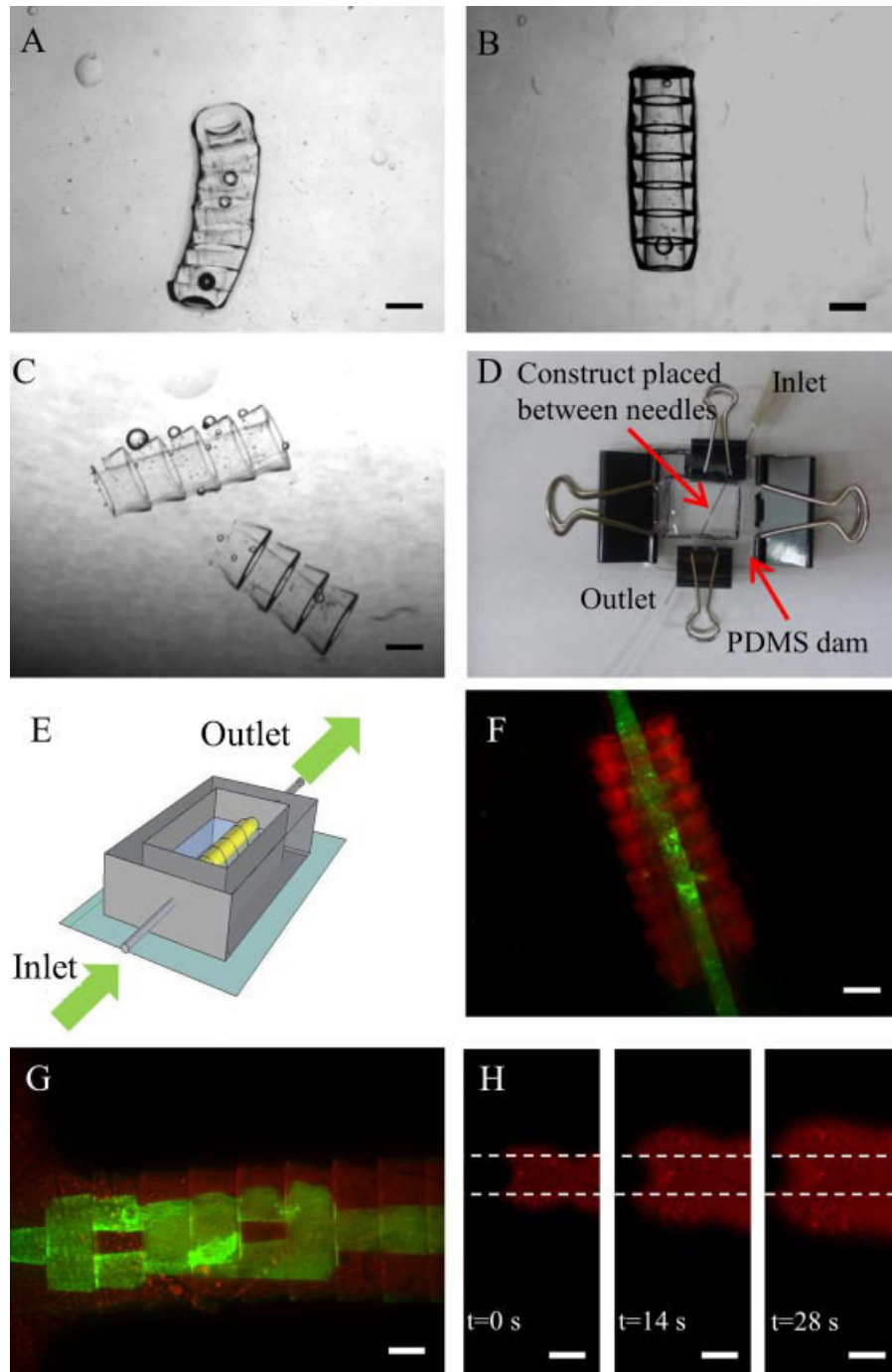
Figure 3. Stabilization and perfusion of the tubular microgel assembly. (**A–C**) Phase images of the stabilized tubular microgel assembly after UV secondary crosslinking when the microgel building blocks were washed by a solution containing: (A) 10% PEG prepolymer, (B) PI (1% in DPBS) or (C) DPBS, respectively, before assembly; (**D**) photograph of the perfusion platform. **E**: Schematic of the perfusion chamber. The perfusion platform is mainly comprised of a PDMS enclosure as a reservoir for microgels and two needles inserted into the two ends of the microgel assembly, functioning as inlet and outlet, respectively; (**F–G**) Perfusion of the stabilized tubular microgel assembly with single or branching lumens by a suspension of green fluorescent microbeads in DPBS; (**H**) sequence of florescent images taken at three different times of the transport of fluorescent dye (Rhodamine) radially across the microgel assembly as it was perfused through the lumen of the microgel assembly. The area in between the dashed lines is the lumen of the assembled construct. Scale bar: 500 μm.

occurred is suggestive that it was not a purely diffusive behavior and may have been aided by a convective process. Further studies in this behavior are currently ongoing in our laboratory.

Sequential Assembly of Cell-Laden Microgels

To validate the use of the sequential assembly process for biomedical applications, we encapsulated NIH-3T3 fibroblasts

within PEG microgels and confirmed the viability of cells by using a viability assay. To further characterize this process, we analyzed the effects of each step in the microgel assembly process (Fig. 4A–E). Three samples from each condition were used for quantification of cell viability. We observed that none of the steps resulted in a significant amount of cell death to the encapsulated NIH-3T3 fibroblasts, similar to previously published studies (Nguyen and West, 2002; Weber et al., 2006). Moreover, it was observed that cell viability of ∼90% was remained after 2 days in culture media (Fig. 4F). The obtained results showed the cell-friendly feature of this assembly approach and serves to validate the use of this assembly process for biological applications. Long-term cell viability (>2 days) was not determined since cells are immobilized in a non-degradable PEG within which they cannot proliferate. The slight loss of cell viability may be due to water-soluble contaminants derived from the hydrophobic phase and the duration of UV exposure during each crosslinking step.

Building Vascular-Like Construct Containing Layers of HUVEC and SMC by Assembling Concentric Microgels

To show the feasibility of fabricating biomimetic vasculature, we generated a concentric design for the microgel building blocks to emulate the two most inner layers of arteries (Jones, 1979; Stegemann et al., 2007). Concentric microgels were fabricated by sequential photocrosslinking through two overlaying masks (Fig. 5A). Concentric microgels with internal layer stained with Nile Red and external layer stained with green florescent microbeads were
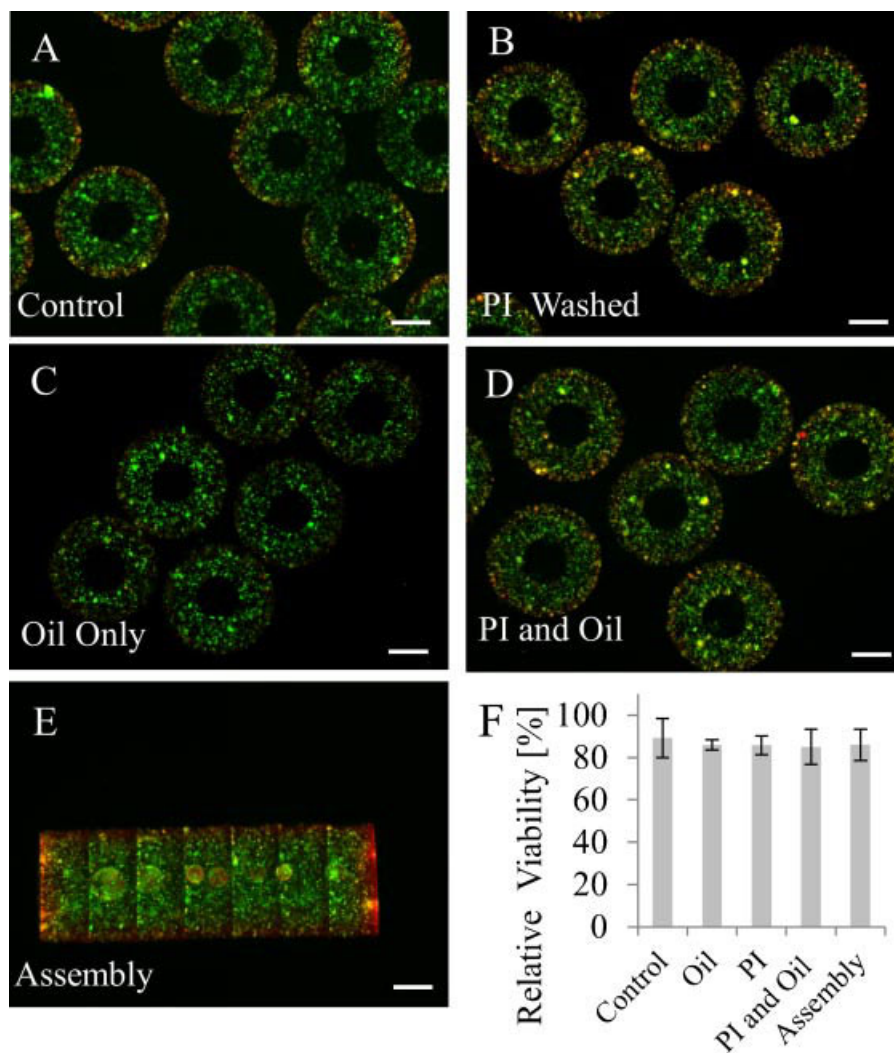

Figure 4. Viability tests for the cell-laden tubular hydrogels as a function of the steps in the assembly process. The sequential assembly procedure was shown to be cell-friendly as demonstrated by viability tests for: (**A**) 3T3 fibroblast-laden microgels; (**B**) microgels washed three times with PI (1% in DPBS); (**C**) microgels exposed to oil; (**D**) microgels exposed to both PI and oil; (**E**) microgel assembly after 2 days in culture medium; (**F**) quantification of samples ($n = 3$) after each fabrication step showed that the assembly process did not result in a significant loss of cell viability. Scale bar: 500 μm.
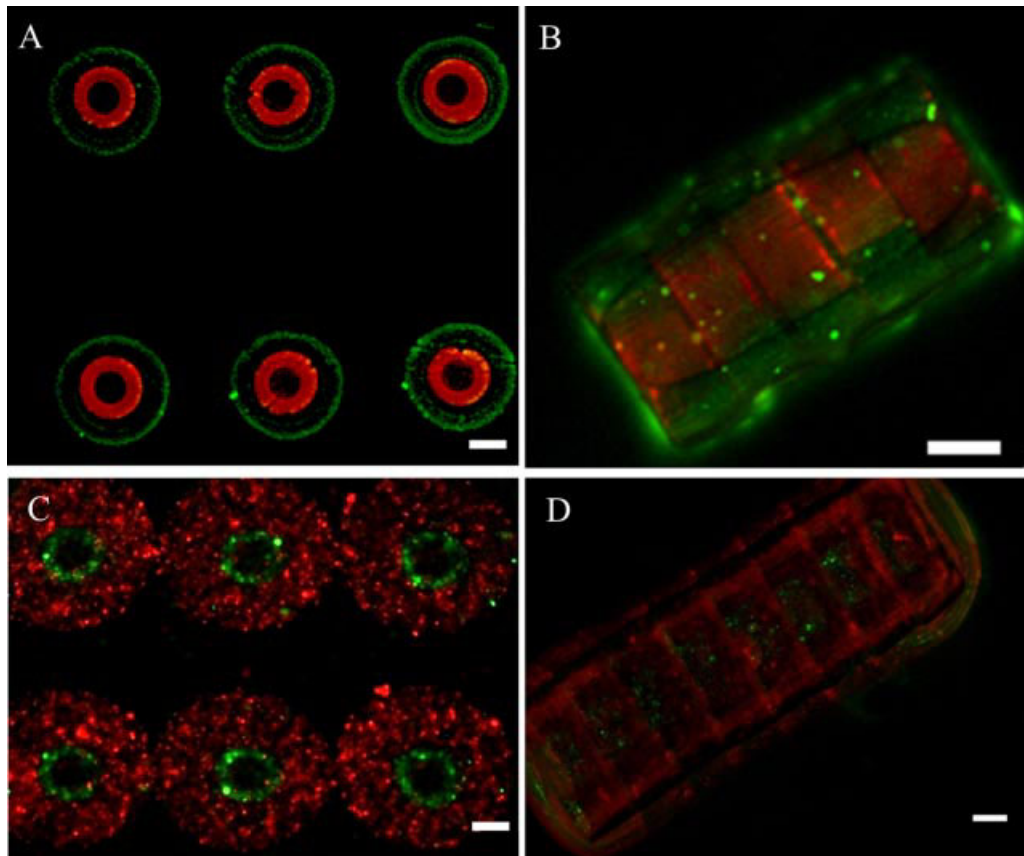
Figure 5. Fabrication of 3D concentric hydrogel constructs by sequential photolithography and assembly of structures containing endothelial and smooth muscle cells. **A,B**: Fluorescence images of the concentric microgel arrays labeled with Nile red (inner ring) and green florescent microbeads (outer ring) and their assembly; (**C,D**) Fluorescence images of the cell-laden concentric microgel arrays and assembly with endothelial cell-laden inner ring (green) and smooth muscle cell-laden outer ring (red). Scale bar: 100 μm.

fabricated and assembled into tubular construct in oil (Fig. 5B). As the first attempt toward building tissue engineered construct mimicking the native vasculature, SMCs, and HUVECs were encapsulated in the external and internal layers of the microgel, respectively (Fig. 5C) and the tubular constructs upon assembly exhibited architecture with physiology-relevant arrangement (Fig. 5D).

Building Assembled Constructs With Different Architecture Using the Assembly Method

To show that the assembly method can be applied to microgels with complex architecture microgels with cross (lock) (Fig. 6A) and donut (key) shapes were fabricated and successfully assembled in oil (Fig. 6B). Moreover, microgels with rectangular cross section were assembled in oil (Fig. 6C). Stacking multiple microgels on top of each other within few seconds shows that this method could potentially be used as a substitute method for other current stacking methods. Green and red labeled microgels were assembled in an alternating manner (Fig. 6D) to show the increased

level of control over the architecture of the assembled constructs.

Discussion

Despite the great progress in the emerging field of "modular" or bottom-up tissue engineering, assembling modular tissues with specific microarchitectures into larger tissue blocks has remained a great challenge (Nichol and Khademhosseini, 2009). There still exists a lack of effective and simple approach to construct 3D tissues with a functional vascular network. As an initial attempt to construct biomimetic 3D vasculature, in this work, we developed a sequential assembly approach that takes advantage of the predefined localization of the microgel units in the microgel arrays and the tendency of hydrophilic PEG microgels to assemble to larger blocks when placed in proximity in hydrophobic environment such as mineral oil. We chose PEG hydrogel as the bulk materials since PEG is biocompatible and exhibits mechanical properties similar to those of soft tissues which makes it qualified for vascular
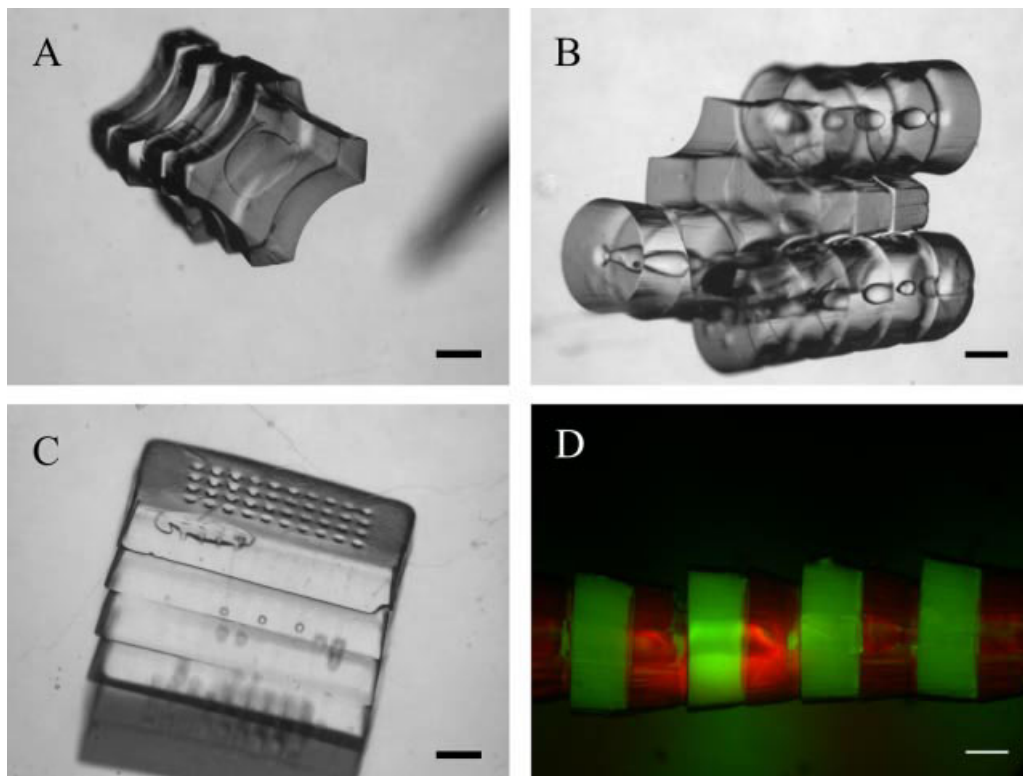
Figure 6. Assembly of microgels with varying shapes. **A**: Phase image of cross-shaped microgel assemblies; **(B)** Phase images of the lock-and-key microgel assembly after secondary assembly; **(C)** Phase image of rectangular shaped porous microgel assemblies; **(D)** Fluorescence image of tubular microgel assembly with alternating green-labeled (green florescent microbeads) and red-labeled (Streptavidin Rhodamine conjugated) microgel building blocks; Scale bar: 500 μm.

tissue engineering (Nguyen and West, 2002). Furthermore, PEG hydrogels demonstrate low levels of cytotoxicity and elicit almost no immunogenic response (Gombotz et al., 1991). Although PEG microgels used here are not biodegradable, bioactive and proteolytic components (i.e., RGD peptide and Matrix metalloproteinase (MMP)-sensitive motif) can be incorporated to improve its properties (Lutolf et al., 2003; Nichol et al., 2010).

In comparison with previously established assembly approaches (Du et al., 2008; McGuigan and Sefton, 2006), the sequential assembly presented in this work exhibits better control over the relative spatial arrangement of different building blocks and overall architecture of the final assembly. Moreover, the size of assembled structure can be easily regulated through controlling the total number of the microgel units in the microgel array. Although the assembly process was performed manually in this study, the entire procedure can be automated to improve the stability and efficiency. In the current approach, the length of the assembled vessels equals to "the thickness of one microgel building block" multiplied by "the number of the microgel building blocks within the assembly." The thickness of one microgel building block cannot be further increased due to the limited penetration of the UV light for crosslinking. The number of microgel building blocks within the assembly can

be increased tremendously by adding more building block designs in the photomask along the direction of the assembly which result in more building blocks available to be assembled. It is foreseen that the current manual assembly process will make it difficult to assemble a large number of microgel building blocks due to the relative instability of manual manipulation and an automated system as proposed above will be very useful to consistently obtain longer microgel assembly. For example, to perform the directional movement of the needle, we could design a direct current (DC)-motor generator attached to a converter that transforms the rotational motion of the motor to translational movement of the needle.

We demonstrated preliminary application of the sequential assembly to fabricate vascular-like constructs with double layers containing endothelial cells and smooth muscle cells. Future work will focus on performing long-term perfusion culture to develop mature vasculature and characterizing its functions. We expect the maturation of the vasculature inside the hydrogel requires dynamic remolding of the cells. Therefore, we would try to use more bioactive hydrogel such as biodegradable PEG or photocrosslinkable gelatin with chemical and mechanical properties better mimic the extracellular matrices (Nichol et al., 2010). The ability of this approach to create constructs with an intrinsic

vascular network potentially offer solutions to tackle one of the most challenging issues in tissue engineering, namely vascularization of larger tissue constructs (Khademhosseini et al., 2009).

Besides our main interests in vascular systems, the sequential assembly can also be used as a general biofabrication method for building hydrogel construct containing multiple cell types with defined physiological architectures and functions. For example, cardiac muscle progenitor cells could be encapsulated in cylindrical microgels made from biodegradable PEG or gelatin to mimic the native muscle fiber. With the embedded vascular-like network, the assembled tissue construct can be further cultured under perfusion for developing functional muscle tissue in vitro.

Conclusion

In summary, we have developed a directed bottom–up approach that could potentially be used for engineering tissue-like constructs with an embedded vascular network. The sequential assembly process enables the spatial control of the individual components within the final assembled construct in a preprogrammed manner. Microengineered hydrogels with internal microchannels were assembled into a tubular construct with multi-level interconnected lumens. Parameters governing the assembly process were examined and conditions were determined that maintained the viability of the encapsulated cells. These data suggest that the assembly method could be used for engineering tissue constructs with 3D vascular network and other complex architectures with physiological relevance.

References

Andersson H, van den Berg A. 2004. Microfabrication and microfluidics for tissue engineering: State of the art and future opportunities. Lab Chip 4(2):98–103.

Borenstein JT, Tupper MM, Mack PJ, Weinberg EJ, Khalil AS, Hsiao J, Garcia-Cardena G. 2010. Functional endothelialized microvascular networks with circular cross-sections in a tissue culture substrate. Biomed Microdevices 12(1):71–79.

Carmeliet P, Jain RK. 2000. Angiogenesis in cancer and other diseases. Nature 407(6801):249–257.

Choi NW, Cabodi M, Held B, Gleghorn JP, Bonassar LJ, Stroock AD. 2007. Microfluidic scaffolds for tissue engineering. Nat Mater 6(11):908–915.

Chrobak KM, Potter DR, Tien J. 2006. Formation of perfused, functional microvascular tubes in vitro. Microvasc Res 71(3):185–196.

Du Y, Lo E, Ali S, Khademhosseini A. 2008. Directed assembly of cell-laden microgels for fabrication of 3D tissue constructs. Proc Natl Acad Sci USA 105(28):9522–9527.

Fiddes LK, Raz N, Srigunapalan S, Tumarkan E, Simmons CA, Wheeler AR, Kumacheva E. 2010. A circular cross-section PDMS microfluidics system for replication of cardiovascular flow conditions. Biomaterials 31(13):3459–3464.

Golden AP, Tien J. 2007. Fabrication of microfluidic hydrogels using molded gelatin as a sacrificial element. Lab Chip 7(6):720–725.

Gombotz WR, Wang GH, Horbett TA, Hoffman AS. 1991. Protein adsorption to poly(ethylene oxide) surfaces. J Biomed Mater Res 25(12):1547–1562.

Hacking SA, Khademhosseini A. 2009. Applications of microscale technologies for regenerative dentistry. J Dent Res 88(5):409–421.

Jen-Huang H, Jeongyun K, Nitin A, Arjun PS, Joseph EM, Arul J, Victor MU. 2009. Rapid fabrication of bio-inspired 3D microfluidic vascular networks. Adv Mater 21(35):3567–3571.

Jones PA. 1979. Construction of an artificial blood vessel wall from cultured endothelial and smooth muscle cells. Proc Natl Acad Sci USA 76(4):1882–1886.

Khademhosseini A, Langer R, Borenstein J, Vacanti JP. 2006. Microscale technologies for tissue engineering and biology. Proc Natl Acad Sci USA 103(8):2480–2487.

Khademhosseini A, Vacanti J, Langer R. 2009. Progress in tissue engieering. Sci Am 300(5):64–71.

Ling Y, Rubin J, Deng Y, Huang C, Demirci U, Karp JM, Khademhosseini A. 2007. A cell-laden microfluidic hydrogel. Lab Chip 7(6):756–762.

Lovett M, Lee K, Edwards A, Kaplan DL. 2009. Vascularization strategies for tissue engineering. Tissue Eng Part B Rev 15(3):353–370.

Lutolf MP, Lauer-Fields JL, Schmoekel HG, Metters AT, Weber FE, Fields GB, Hubbell JA. 2003. Synthetic matrix metalloproteinase-sensitive hydrogels for the conduction of tissue regeneration: Engineering cell-invasion characteristics. Proc Natl Acad Sci USA 100(9):5413–5418.

McGuigan AP, Sefton MV. 2006. Vascularized organoid engineered by modular assembly enables blood perfusion. Proc Natl Acad Sci USA 103(31):11461–11466.

Menolascina F, Bellomo D, Maiwald T, Bevilacqua V, Ciminelli C, Paradiso A, Tommasi S. 2009. Developing optimal input design strategies in cancer systems biology with applications to microfluidic device engineering. BMC Bioinformatics 10(Suppl 12):S4.

Mironov V, Visconti RP, Kasyanov V, Forgacs G, Drake CJ, Markwald RR. 2009. Organ printing: Tissue spheroids as building blocks. Biomaterials 30(12):2164–2174.

Nguyen KT, West JL. 2002. Photopolymerizable hydrogels for tissue engineering applications. Biomaterials 23(22):4307–4314.

Nichol JW, Khademhosseini A. 2009. Modular tissue engineering: Engineering biological tissues from the bottom up. Soft Matter 5(7):1312–1319.

Nichol JW, Koshy ST, Bae H, Hwang CM, Yamanlar S, Khademhosseini A. 2010. Cell-laden microengineered gelatin methacrylate hydrogels. Biomaterials 31(21):5536–5544.

Shi Z, Chen N, Du Y, Khademhosseini A, Alber M. 2009. Stochastic model of self-assembly of cell-laden hydrogels. Phys Rev E Stat Nonlin Soft Matter Phys 80(6 Pt 1):061901.

Shin M, Matsuda K, Ishii O, Terai H, Kaazempur-Mofrad M, Borenstein J, Detmar M, Vacanti JP. 2004. Endothelialized networks with a vascular geometry in microfabricated poly(dimethyl siloxane). Biomed Microdevices 6(4):269–278.

Stegemann JP, Kaszuba SN, Rowe SL. 2007. Review: Advances in vascular tissue engineering using protein-based biomaterials. Tissue Eng 13(11):2601–2613.

van der Meer AD, Poot AA, Duits MH, Feijen J, Vermes I. 2009. Microfluidic technology in vascular research. J Biomed Biotechnol 2009:823148.

Visconti RP, Kasyanov V, Gentile C, Zhang J, Markwald RR, Mironov V. 2010. Towards organ printing: Engineering an intra-organ branched vascular tree. Expert Opin Biol Ther 10(3):409–420.

Weber LM, He J, Bradley B, Haskins K, Anseth KS. 2006. PEG-based hydrogels as an in vitro encapsulation platform for testing controlled beta-cell microenvironments. Acta Biomater 2(1):1–8.

Whitesides GM. 2006. The origins and the future of microfluidics. Nature 442(7101):368–373.